Determination of optical parameters on knee bending of the feet using fiber optic

Ade Fitri*, Wahyu Candra, Bunga Meyzia

Department of Physics, Universitas Riau, Pekanbaru 28293, Indonesia

ABSTRACT

Fiber optics are the right transmission medium to monitor the movement of the human body, one of them is knee activity. Single-mode fiber (SMF) and fiber Bragg grating (FBG) as sensing sensors that can monitor damage to bad conditions of the human joint area so can prevent further damage. The purpose of this study was to design fiber optic-based belts due to macrobending with sinusoidal patterns, determine the relationship of knee benders with average power change of SMF and FBG, measure changes in power loss (L) fiber optics as a function of optical fiber diameter (d) and knee angle, and determine the optimum sensitivity (S) of SMF and FBG in detecting knee bending. The results showed that L of 0.0751 dB and S of 0.017442 dB are the largest values produced from the SMF belt with values d of 12 mm and knee angle of 180°. The values L of 2.0177 dB and S of 0.591382 dB are the largest values produced from FBG belts with values d of 8 mm and knee angle of 180°. The results of this study explain that FBG is more effective to use because it has a higher S value than SMF.

* Corresponding Author
E-mail address: ade.fitri2330@student.unri.ac.id

1. INTRODUCTION

The knee joint is a 'hinge type' synovial joint with the movement of flexion and extension combined with rotation and shear. The knee joint is a joint capable of withstanding heavy axial loading. The anatomy of the knee joint is composed of several tissues, namely bone components, soft tissue components, nervous tissue, and vascular tissue [1, 2]. Complaints, when someone goes up and downstairs, can be caused by osteoarthritis. The development of a health monitoring application device at a relatively low cost is an important effort to monitor the poor condition of the human joint area which can prevent further damage [3-5]. Knee activity monitoring applications, gait asymmetric detection can be used to indicate the condition of the knee joint [6, 7]. Fiber optic sensor devices are good for monitoring knee movement activities because of their various advantages such as resistance to electromagnetic interference, low cost, lightweight components, and ease of application in the sensor [8-10].

Single-mode fiber (SMF) and fiber Bragg grating (FBG) are of further concern because of their high precision and accuracy [11]. SMF is able to carry signals in one channel which is quite long [12]. Based on the use of optical fiber as a transmission medium, there are losses caused by intrinsic and extrinsic factors [13]. Intrinsic factors of optical fiber such as absorption (absorption loss) and scattering (rayleigh scattering loss), extrinsic factors such as bending loss, splicing loss, coupling loss [14-16].

This study presents the determination of optical parameters for knee bending using optical fiber using a laser diode as a light source with a wavelength of 1310 nm which propagates inside the SMF and FBG sensors while the optical power output of the optical fiber is detected using optical power meter (OPM). SMF and FBG sensors are modulated in such a way on elastic material belts with variations in the diameter of the sinusoidal pattern and variations in the bending of the knee-leg angle,

making it much easier and more cost-effective. After getting all the data, analysis and calculations were carried out in order to obtain and find out a better sensitivity value between SMF and FBG.

2. DESIGN OF FBG ON KNEE KINEMATICS AND DYNAMICS

Optical fiber is a transparent medium made of thin glass, plastic, or polymer fibers used to transmit light signals from one place to another. Part of the optical fiber consists of coating, cladding, and core [17-20]. In general, optical fiber is divided into several types [21]. SMF has the advantage of better performance such as, in channel attenuation and bandwidth usage [22]. Multimode optical fiber has a narrow bandwidth, poor transmission, and small transmission capacity. FBG is a type of fiber optic sensor that is used as a temperature and strain sensor. The Bragg wavelength value of the FBG is obtained as follows:

$$\lambda_B = 2\, n_{eff} \Lambda \tag{1}$$

Power reduction in optical fiber occurs due to a leak or lack of clarity of material from an optical fiber. The causes of power reduction in optical fiber are absorption, scattering, and bending losses. Bending is a bending that causes the light that propagates in an optical fiber to deviate from the direction of its transmission. In this study, the loss is focused on bending loss for macrobending. Macrobending occurs when light passes through an optical fiber that is bent to form a curvature with a radius greater than the radius of the optical fiber. Microbending is caused by the difference in the rate of expansion and shrinkage between the optical fiber and its outer shield (coating).

The knee is a complex hinge joint with the greatest flexion and extension in the sagittal plane and varus and valgus rotation in the frontal plane. The knee has a role in maintaining stability and control during various loading situations. A collection of lower limb joints that play a role in body movement (knees, ankles, and hips) the knee is one of the most susceptible to disorders such as osteoarthritis [23, 24]. Osteoarthritis is a joint disorder characterized by cell stress and extracellular matrix degradation and is characterized by cartilage degradation, osteophyte formation, joint inflammation, pain, and loss of normal joint function. A person's limitations in the activity of going up and downstairs are caused by a person's inability to support the weight. When a person climbs and descends the stairs the load received by the knees is 3–4 times the body weight. Cartilage degeneration in the joints causes osteokinematic and arthrokinematic disorders of the joints.

On the inside of the belt are glued optical fibers in the form of SMF and FBG with $\lambda = 1310$ nm and $P_0 = -5$ dBm given alternately sinusoidal pattern diameters (d)are 8 mm, 10 mm, and 12 mm. Input power (P_0) is sourced from the diode laser and the output power for the initial power (P_i) and final power (P_f) will be read in the OPM. The belt that has been given a sinusoidal diameter pattern is attached to the knee of the object's leg. The object consists of a woman with a large variation of the knee angle used is 30°. The age of the object is 22 years. In the study, the belts were alternated between SMF and FBG. The object is measured while sitting on a chair in order to facilitate bending of the object's knees and measurements are also taken when the object is climbing the stairs to see how much angle will be formed and how much power is lost to climb each ladder.

3. ANALYSIS OF FBG PROPERTIESON KNEE BENDING

Before the belt is attached to the object's legs, the value of the initial output power will be measured when the SMF and FBG belts are stretched straight on the floor. The P_i values with d of 8 mm, 10 mm, and 12 mm for SMF are -6.95 dBm, -6.94 dBm, and -6.88 dBm, while for FBG are -6.73 dBm, -7.08 dBm, and -6.77 dBm. The end of the optical fiber is connected to the input and output in the form of a laser diode and OPM. Objects with a sitting position and their knees will be bent with a certain variation 30°, 60°, 90°, 120°, 150°, and 180° will be monitored and recorded its $P_f$using delta in general, namely:

$$\overline{\Delta P} = \overline{P_f} - \overline{P_i} \tag{2}$$

where $\overline{\Delta P}$ is the average power change of 5 repetitions, $\overline{P_f}$ is the average final power after the belt is attached to the object's foot, and $\overline{P_i}$ is the initial power after the belt is paired with a sinusoidal pattern and the graph in the following figure is obtained.
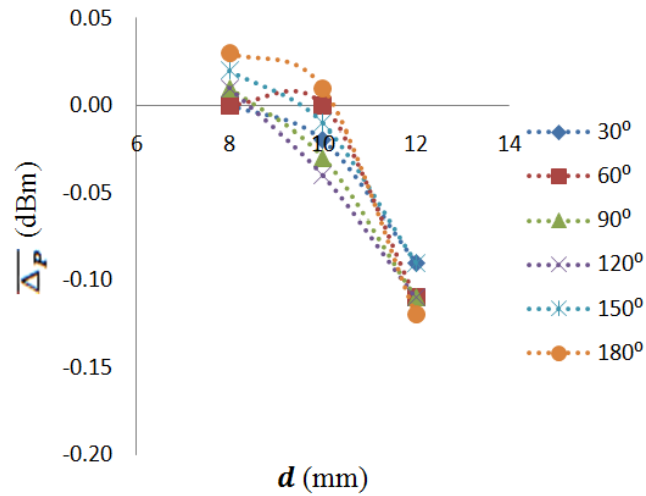

Figure 1. The graph $\overline{\Delta P}$ of SMF against d and θ_k.

Figure 1 shows that $\overline{\Delta P}$ value of SMF with respect to d and θ_k has the smallest $\overline{\Delta P}$ value found at $d = 12$ mm and $\theta_k = 180°$ with a value of $\overline{\Delta P} = -0.12$ dBm. The largest $\overline{\Delta P}$ value of SMF is at $d = 8$ mm and $\theta_k = 180°$ with a value of $\overline{\Delta P} = 0.03$ dBm. In this study, the larger the diameter of the curvature used, the smaller the difference in output power, which means the smaller the light that can be transmitted. Figure 2 presents that $\overline{\Delta P}$ value of FBG to d and θ_k has the smallest $\overline{\Delta P}$ value found at $d = 8$ mm and $\theta_k = 180°$ with a value of $\overline{\Delta P} = -3.98$ dBm. The largest $\overline{\Delta P}$ value of FBG is at $d = 12$ mm and $\theta_k = 30°$ with a value of $\overline{\Delta P} = -0.20$ dBm. In this study, the larger the diameter of the curvature used, the greater the difference in output power produced.
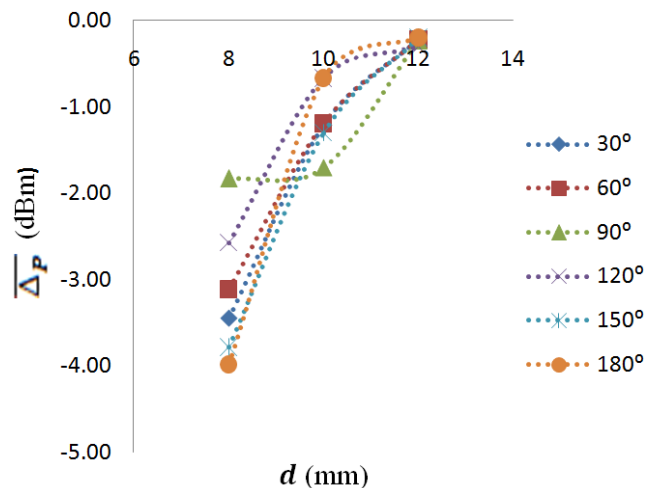

Figure 2.The graph $\overline{\Delta P}$ of FBG against d and θ_k.

The value of power loss (L) is closely related to the value of power. Calculations are carried out using the equation:
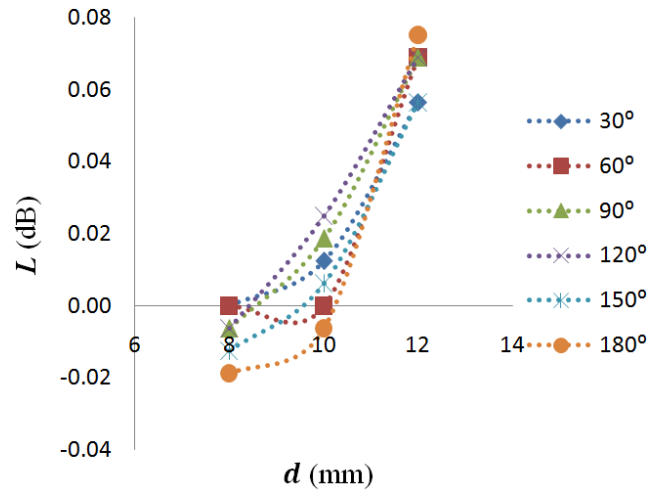
$$L = 10\ LOG\ \frac{\overline{P_f}}{\overline{P_i}}$$ (3)

Figure 3. The graph L of SMF against d and θ_k.

Figure 3 describes the L value of SMF against d and θ_k seems like a small diameter of curvature $d = 8$ mm has a smaller power loss value of-0.0188 dBwhen compared with the diameter of 10 mm and 12 mm. While $d = 12$ mm has the largest power loss value among the three diameters, which is 0.0751 dB.The value of power loss in SMF optical fiber in this study is caused by the bending factor. Figure 4 illustrates the value L of FBG against d and θ_k, it can be seen that the small diameter of curvature $d = 8$ mm has a larger power loss value of 2.0177 dB when compared with the diameter of 10 mm and 12 mm. Meanwhile, $d = 12$ mm has the smallest power loss among the three diameters, which is 0.1264 dB. This is because the diameter of the bend 12 mm has an output power that is almost close to the initial output power, thus causing the difference in output power to be smaller than the diameter of 8 mm and 10 mm.
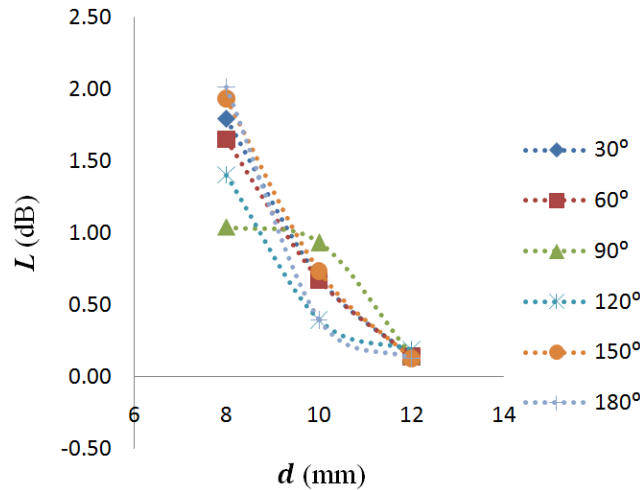

Figure 4. The graph L of FBG against d and θ_k.

From the calculation of the L values carried out on SMF and FBG, the largest L value for SMF is $d = 12$ mm and the largest L value for FBG is $d = 8$ mm. This is different because it is affected by the sensitivity of the optical fiber. One study states that the L value is greater if the d value is reduced [25]. In this study, it can be said that FBG is more sensitive than SMF. To prove the sensitivity value of the optical fiber, it is calculated using the equation:

$$s = \frac{\overline{\Delta P}}{\overline{P_l}} = \frac{\overline{P_f} - \overline{P_l}}{\overline{P_l}} \tag{4}$$

In this study, 3 variations of diameter were used, namely 8 mm, 10 mm, and 12 mm. From the results of observations and calculations, it is found that the sensitivity value on SMF is found in the curvature of the diameter of 12 mm with a value for each angle, namely 0.013081, 0.015988, 0.015988, 0.015988, 0.013081, 0.017442 while the sensitivity of FBG is at a diameter of 8 mm, namely 0.511144, 0.46211, 0.271917, 0.381872, 0.561664 and 0.591382. Based on the sensitivity value, we can conclude that a more effective optical fiber is found in FBG optical fiber with $d = 8$ mm.

4. CONCLUSION

Variations in bending diameter cause different output power and power loss for SMF and FBG. The value of $L = 0.0751$ dB and $S = 0.017442$ dB is the largest value generated from the SMF belt with a value of $d = 12$ mm and $\theta_k = 180°$, in SMF the L value of optical fiber will increase with the increasing d value and bending θ_k at the knee of the leg. The value of $L = 2.0177$ dB and $S = 0.591382$ dB is the largest value generated from the FBG belt with a value of $d = 8$ mm and $\theta_k = 180°$. In FBG, the L value of optical fiber will increase as it gets smaller dvalue optical fiber used. The FBG is more effective to use because it has a higher S value than SMF.

REFERENCES

[1]   Perera, K., Ivone, R., Natekin, E., Wilga, C. A., Shen, J., & Menon, J. U. (2021). 3D bioprinted implants for cartilage repair in intervertebral discs and knee menisci. *Frontiers in Bioengineering and Biotechnology*, **9**, 754113.

[2]   Trávníčková, M. & Bačáková, L. (2018). Application of adult mesenchymal stem cells in bone and vascular tissue engineering. *Physiol Res*, **67**(6), 831–850.

[3]   Faisal, A. I., Majumder, S., Mondal, T., Cowan, D., Naseh, S., & Deen, M. J. (2019). Monitoring methods of human body joints: State-of-the-art and research challenges. *Sensors*, **19**(11), 2629.

[4]   Zhang, J., Tian, G. Y., Marindra, A. M., Sunny, A. I., & Zhao, A. B. (2017). A review of passive RFID tag antenna-based sensors and systems for structural health monitoring applications. *Sensors*, **17**(2), 265.

[5]   Soerbakti, Y., Syahputra, R. F., Saktioto, S., & Gamal, M. D. H. (2020). Investigasi kinerja antena berdasarkan dispersi anomali metamaterial struktur heksagonal split ring resonator. *Komunikasi Fisika Indonesia*, **17**(2), 74–79.

[6]   Salim, G. M. & Zawawi, M. A. (2018). Knee joint movement monitoring device based on optical fiber bending sensor. *Journal of Telecommunication, Electronic and Computer Engineering (JTEC)*, **10**(1-3), 25–29.

[7]   Anwary, A. R., Yu, H., & Vassallo, M. (2018). An automatic gait feature extraction method for identifying gait asymmetry using wearable sensors. *Sensors*, **18**(2), 676.

[8]   Leal-Junior, A. G., Diaz, C. A., Avellar, L. M., Pontes, M. J., Marques, C., & Frizera, A. (2019). Polymer optical fiber sensors in healthcare applications: A comprehensive review. *Sensors*, **19**(14), 3156.

[9]   Butt, A. M. & Qureshi, K. K. (2019). Smart lower limb prostheses with a fiber optic sensing sole: A multicomponent design approach. *Sensors and Materials*, **31**.

[10]   Saktioto, T., Ramadhan, K., Soerbakti, Y., & Irawan, D. (2021). Integration of chirping and apodization of Topas materials for improving the performance of fiber Bragg grating sensors. *Journal of Physics: Conference Series*, **2049**(1), 012001.

[11]   Sahota, J. K., Gupta, N., & Dhawan, D. (2020). Fiber Bragg grating sensors for monitoring of physical parameters: A comprehensive review. *Optical Engineering*, **59**(6), 060901.

[12]   Shariati, B., Mastropaolo, A., Diamantopoulos, N. P., Rivas-Moscoso, J. M., Klonidis, D., & Tomkos, I. (2018). Physical-layer-aware performance evaluation of SDM networks based on SMF bundles, MCFs, and FMFs. *Journal of Optical Communications and Networking*, **10**(9), 712–722.

[13]   Richardson, D. J. (2016). New optical fibres for high-capacity optical communications. *Philosophical Transactions of the Royal Society A: Mathematical, Physical and Engineering Sciences*, **374**(2062), 20140441.

[14] Tut Tahira, K., Omar Faruk, M., Ruma, T. A., Saha, T., & Rahman, M. M. (2019). Analysis of fiber loss mechanisms in communication system to simulate different attenuation. *Journal of Engineering Research and Reports*, **8**(1), 1–15.

[15] Saktioto, T., Fadilla, F. D., Soerbakti, Y., & Irawan, D. (2021). Application of fiber Bragg grating sensor system for simulation detection of the heart rate. *Journal of Physics: Conference Series*, 2049(1), 012002.

[16] Husein, I. R., Nawi, N. D., & Hairi, H. M. (2021). Electrical discharge of butane and propane for carbon plasma with air impurities, slightly ionized at high pressure. *Science, Technology and Communication Journal*, **1**(3), 109–116.

[17] Saktioto, Zairmi, Y., Veriyanti, V., Candra, W., Syahputra, R. F., Soerbakti, Y., Asyana, V., Irawan, D., Okfalisa, Hussein, N. A., Syamsudhuha, & Anita, S. (2020). Birefringence and polarization mode dispersion phenomena of commercial optical fiber in telecommunication networks. *Journal of Physics: Conference Series*, **1655**(1), 012160.

[18] Ramadhan, K., Saktioto, Syahputra, R. F., Soerbakti, Y., & Fauzan, M. (2020). Dispersi multi-layer pada inti serat optik moda tunggal. *Seminar Nasional Fisika Universitas Riau V (SNFUR-5) 2020*, **5**, 1–5.

[19] Ramadhan, K. & Saktioto, S. (2021). Integrasi chirping dan apodisasi bahan TOPAS untuk peningkatan kinerja sensor serat kisi Bragg. *Indonesian Physics Communication*, **18**(2), 111–123.

[20] Fadilla, F. D. & Saktioto, S. (2021). Aplikasi sistem sensor fiber bragg grating untuk pendeteksian simulasi denyut jantung. *Indonesian Physics Communication*, **18**(2), 151–158.

[21] Roslan, M. S., Chaudhary, K. T., & Mazalam, E. (2020). Overview of temporal soliton transmission on photonic crystal fiber and nanowires. *Science, Technology and Communication Journal*, **1**(1), 15–18.

[22] Mrabet, H., Dayoub, I., Haxha, S., & Attia, R. (2019). Performance analysis of 2D-OCDMA system in long-reach passive optical network. *Optics & Laser Technology*, **117**, 64–72.

[23] Katz, J. N., Arant, K. R., & Loeser, R. F. (2021). Diagnosis and treatment of hip and knee osteoarthritis: a review. *JAMA*, **325**(6), 568–578.

[24] Mani, E., Tüzün, E. H., Angın, E., & Eker, L. (2020). Lower extremity proprioceptive sensation in patients with early stage knee osteoarthritis: A comparative study. *The Knee*, **27**(2), 356–362.

[25] Petersen, C. R., Engelsholm, R. D., Markos, C., Brilland, L., Caillaud, C., Trolès, J., & Bang, O. (2017). Increased mid-infrared supercontinuum bandwidth and average power by tapering large-mode-area chalcogenide photonic crystal fibers. *Optics Express*, **25**(13), 15336–15348.